ISBN: 978-3-95450-210-3 doi:10.18429/JACoW-FEL2019-WEP016

PRECISE LASER-TO-RF SYNCHRONIZATION OF PHOTOCATHODE LASERS

M. Titberidze*, M. Felber, T. Kozak, T. Lamb, J. Müller, H. Schlarb, S. Schulz, F. Zummack
Deutsches Elektronen-Synchrotron, DESY, Hamburg, Germany
C. Sydlo, Paul Scherrer Institut, PSI, Villigen, Switzerland

Abstract

RF photo-injectors are used in various large, mid and small-scale accelerator facilities such as X-ray Free Electron Lasers (XFELs), external injection-based laser-driven plasma accelerators (LPAs) and ultrafast electron diffraction (UED) sources. Many of these facilities require a high precision synchronization of the photo-injector laser system, either because of beam dynamics reasons or the photo-injector directly impacting pump-probe experiments carried out to study physical processes on femtosecond timescales. It is thus crucial to achieve synchronization in the order of 10 fs rms or below between the photocathode laser and the RF source driving the RF gun. In this paper, we present the laser-to-RF synchronization setup employed to lock a commercial near-infrared (NIR) photocathode laser oscillator to a 2.998 GHz RF source. Together with the first results achieving ~ 10 fs rms timing jitter in the measurement bandwidth from 10 Hz up to 1 MHz, we describe an advanced synchronization setup as a future upgrade, promising even lower timing jitter and most importantly long-term timing drift stability.

INTRODUCTION

The (short and innovative bunches and accelerators at DESY) SINBAD facility will host several accelerator research and development experiments like ARES [1] and AXSIS [2]. These experiments will mainly focus on the production of ultra-short electron bunches (0.2 fs to 10 fs) and testing novel high gradient acceleration techniques. The (accelerator research experiment at sinbad) ARES is a conventional S-band linear RF accelerator (linac) which is currently in the construction and commissioning phase [3]. It consists of S-band (f_{RF} = 2.998 GHz) normal conducting accelerating structures: 1.5 cell RF gun [4] and two travelling wave structures (TWS1, TWS2) [5]. The electron bunches are produced by impinging ultrashort laser pulses on a photocathode inside the RF gun.The ARES linac is schematically shown in Fig. 1. The final electron beam parameters at ARES are defined in [3] and require an arrival time jitter of < 10 fs rms. In order to meet this requirement it is crucial to achieve a precise laser-to-RF synchronization between the pulsed injector laser and the 2.998 GHz RF reference signal from the RF master oscillator (MO). The injector laser is a commercial system from Light Conversion[1] with a fundamental wavelength of 1030 nm and variable pulse duration of 0.16 ps to 10 ps. The laser oscillator of this system is designed such that the repetition rate of the optical pulses f_{rep} = 83.28 MHz is the 36$^{\mathrm{th}}$ sub-harmonic of the RF reference frequency f_{RF} = 2.998 GHz.

DIRECT CONVERSION BASED LASER-TO-RF SYNCHRONIZATION

General Concept

One of the most common techniques to synchronize a mode-locked laser to an RF signal is using a fast photodetector [6–9]. The pulsed optical signals are converted to electrical pulses which are composed of high spectral purity harmonics of the laser repetition rate. The cutoff frequency of the RF comb is given by the bandwidth of the photodetector. The desired frequency component of the RF comb can be filtered out using an RF band-pass filter (BPF) and amplified until the signal level is sufficient for downconvertion. The downconverted signal is digitized using an analog-to-digital converter (ADC) employing so called non-IQ sampling [6, 10, 11]. The amplitude and phase information is extracted in the digital domain. The obtained phase error information is fed back to the piezo actuator of the laser oscillator using a piezo driver to establish the phase locked loop (PLL).

There are several advantages of downconverting the photodetected signal to an intermediate frequency (IF) instead of baseband. Baseband signals are often degraded by undesired DC offsets due to imperfections of the electronics and they are highly susceptible to electromagnetic interference (EMI). Both effects limit the overall PLL performance potentially leading to a poor synchronization performance. These problems are mitigated by direct sampling the IF signal and using digital phase detection.

However, there are still fundamental limitations related to the photodetection process, such as the AM-PM effect, where optical power fluctuations are converted to phase fluctuations of each frequency component of the generated frequency comb [12, 13] while low signal levels from the photodetector together with the intrinsic thermal and shot noise sources lead to a limited signal-to-noise ratio (SNR).

One can estimate the thermal noise limited timing jitter for a 50 Ω terminated photodetector using the following expression [14]:

$$T_{\mathrm{rms}} = \frac{1}{2\pi f_{\mathrm{c}}}\sqrt{\frac{P_{\mathrm{th}}}{P_{\mathrm{c}}}\Delta f}. \qquad (1)$$

Here, $P_{\mathrm{th}} = -174$ dBm/Hz is the thermal noise power at room temperature in a 1 Hz bandwidth. P_{c} and f_{c} are the

* mikheil.titberidze@desy.de
[1] Pharos SP-06-200-PP

ISBN: 978-3-95450-210-3 doi:10.18429/JACoW-FEL2019-WEP016

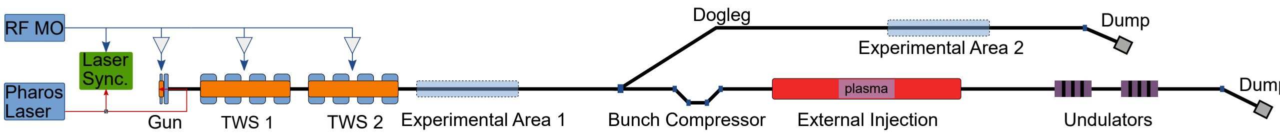

Figure 1: Layout of ARES linac.

carrier power and frequency respectively. Δf is the noise bandwidth. Using a commercial fast photodetector, a carrier power of −25 dBm at 2.998 GHz can be extracted for an average optical power of 5 mW and applied reverse bias voltage of 12 V. This leads to approximately 2 fs thermal noise limited timing jitter in a 1 MHz bandwidth. In addition, the long-term timing drift performance is a major problem in the direct conversion based laser-to-RF synchronization setups. Many RF components involved in the synchronization setup are susceptible to temperature and humidity changes, leading to an unavoidable timing drifts and poor long-term timing stability [15].

Technical Implementation

In this section, technical details of the injector laser synchronization together with the measurement setup (Fig. 2) are discussed. The optical pulse train from the laser oscillator is split by a polarizing beam splitter into two paths. The first path provides the optical pulse train to the direct conversion based laser-to-RF synchronization setup, while the second optical path is reserved for a future upgrade discussed in the next section.

The optical pulse train with an average optical power of ≈ 5 mW is guided to a commercial InGaAs photodetector[2] via a fiber coupled collimator. The photodetected signal is split by the RF splitter (SPL) providing the signals to in-loop and out-of-loop RF chains. The 37$^{\text{th}}$ and 36$^{\text{th}}$ harmonics (3.081 GHz, 2.998 GHz) of the laser oscillator repetition rate are filtered using custom built RF bandpass filters for in-loop and out-of-loop setups respectively. The in-loop setup is dedicated to lock the laser oscillator, while the out-of-loop signal is used for performance evaluation.

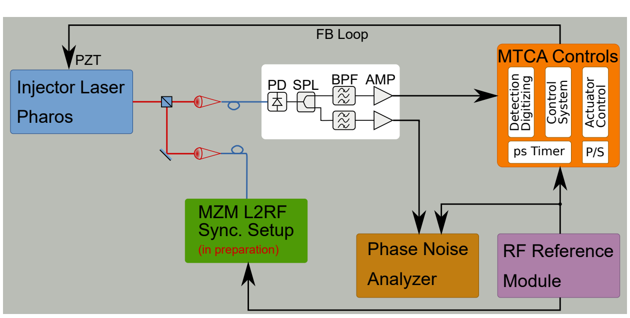

Figure 2: Schematic diagram of the laser oscillator synchronization and out-of-loop measurement setup.

The 3.081 GHz signal is downconverted using the 2.998 GHz RF reference signal resulting in an IF = f_{rep} = 83.28 MHz. The obtained IF is digitized with a sampling rate of $f_s = f_c/24 = 124.92$ MHz. The signal downconversion, digitization and phase feedback is carried out on the MicroTCA.4 electronics platform [16], offering extremly large flexibility for controls compared to conventional analog controllers.

Measurement Results

After successfully locking the laser oscillator to the RF reference signal, the out-of-loop absolute and residual phase-noise measurements have been carried out using a phase-noise analyzer[3] with a measurement bandwidth of 10 Hz to 1 MHz. The phase-noise power spectral densities (PSDs) and corresponding integrated jitters are summarized in Fig. 3 and Fig. 4. Here the green curves depict the absolute phase-noise PSD and the corresponding timing jitter of the RF reference signal. The orange curves show the absolute phase-noise PSD and timing jitter of the locked laser oscillator measured at the 36$^{\text{th}}$ harmonic (2.998 GHz) of the repetition rate.

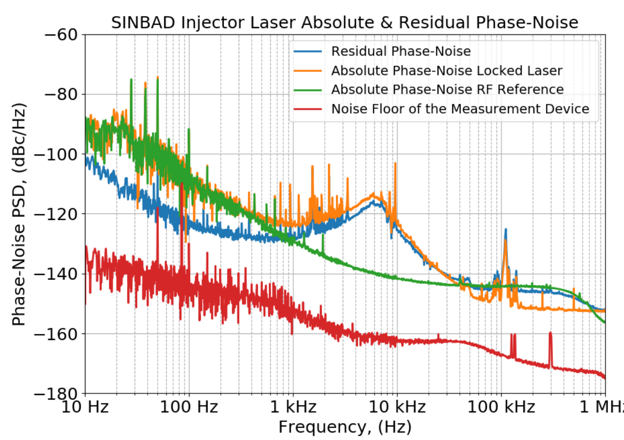

Figure 3: Measured absolute and residual phase-noise power spectral densities.

The overlap of the phase-noise PSD curves (green, orange), indicate that the locking bandwidth of the laser oscillator is about a few kHz. The out-of-loop residual phase-noise measurement between the RF reference and the laser oscillator is depicted by the blue curves in Figs. 3,4. The total integrated timing jitter amounts about 10 fs rms, dominated by the so called "waterbed effect" in the range from 1 kHz to 40 kHz. Beyond 40 kHz the integrated timing jitter is governed by the noise floor of the RF reference. The noise floor of the phase-noise analyzer was measured when both

[2] https://www.eotech.com/, ET3500F

[3] R&S FSWP26

ISBN: 978-3-95450-210-3 doi:10.18429/JACoW-FEL2019-WEP016

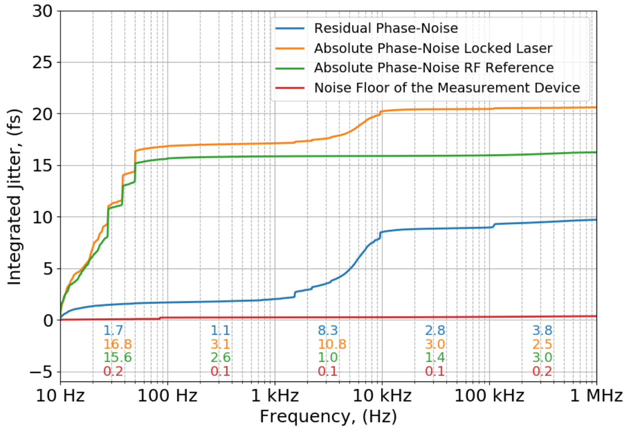

Figure 4: Integrated timing jitter calculated from the phase-noise PSD in Fig 3.

the signal and the external reference were derived from the same source (RF MO). The red curve in Fig. 3 shows the measured noise floor of the phase-noise analyzer amounting 300 as rms in the full measurement bandwidth. The timing jitter contribution added by the measurement device itself is negligible compared to the high frequency noise floors of the RF reference and the laser oscillator.

FUTURE UPGRADE

In order to mitigate the problems associated with the direct conversion based laser-to-RF synchronization setup, it is planned to build a Mach-Zehnder Modulator (MZM) based laser-to-RF synchronization setup [9]. It has been shown in a pilot study that the MZM based laser-to-RF synchronization scheme for S-band frequencies can suppress the AM-PM effect and offer timing jitter and especially drift performance in the order of 10 fs rms [9, 15].

This approach is based on sampling the RF reference signal zero crossings with optical pulses within the integrated MZM. This allows to convert the relative timing error between these two sources into an amplitude modulation of the optical pulses. A sketch for the simplified case is shown in Fig. 5. When the relative timing between the laser oscillator pulse train and the RF reference is zero ($\Delta\varphi = 0$), optical pulses arrive at the zero crossings of the RF reference. Hence, an amplitude modulation of the optical pulses does not take place. When the relative timing between the two sources is not zero ($\Delta\varphi \neq 0$), the amplitude modulation of the laser pulses will occur. For any $\Delta\varphi \neq 0$, each subsequent pair of optical pulses samples opposite slopes of the RF signal. This translates to an amplitude mismatch of the individual laser pulse since they experience positive and negative voltages of the RF signal respectively. The amplitude modulation of the optical pulses in the time domain transfers to the RF spectrum as additional frequency components (orange comb lines in Fig. 5). One can detect the amplitude of one of these modulation frequencies and build a feedback loop in order to establish a PLL between the laser oscillator and the RF reference signal. For more details about the principle of operation of the scheme see [8, 9, 15].

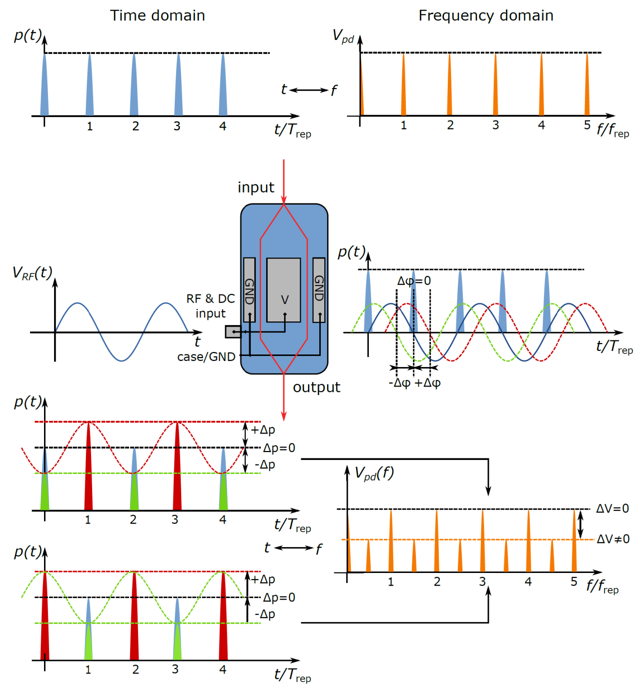

Figure 5: Concept for Mach-Zehnder modulator based laser-to-RF synchronization scheme. Blue pulses indicate the unmodulated optical pulses in time domain, red and green pulses depict the modulated optical pulses in time domain. Orange comb lines show the frequency spectra for both modulated and unmodulated optical pulses.

CONCLUSION

In this paper we have shown the first results of the recently commissioned direct conversion based photo-injector laser-to-RF synchronization setup at the SINBAD facility. The measured timing jitter performance is ≈ 10 fs rms in the bandwidth of 10 Hz to 1 MHz which is sufficient for the initial phase of the experiments planned at ARES and satisfies its design requirements. The MZM based laser-to-RF setup is currently in preperation and commissioning will start in the near future as an upgrade.

REFERENCES

[1] B. Marchetti *et al.*, "Electron-Beam Manipulation Techniques in the SINBAD Linac for External Injection in Plasma Wake-Field Acceleration", *Nucl. Instr. Meth.*, vol. 829, pp. 278–283, 2016. doi.org/10.1016/j.nima.2016.03.041

[2] https://axsis.desy.de/

[3] E. Panofski *et al.*, "Status Report of the SINBAD-ARES RF Photoinjector and LINAC Commissioning", in *Proc. 10th Int. Particle Accelerator Conf. (IPAC'19)*, Melbourne, Australia, May 2019, pp. 906–909. doi:10.18429/JACoW-IPAC2019-MOPTS026

ISBN: 978-3-95450-210-3 doi:10.18429/JACoW-FEL2019-WEP016

[4] M. Hada *et al.*, "REGAE: New Source for Atomically Resolved Dynamics", in *Proc. 2012 Research in Optical Sciences*, Berlin, Germany, Mar. 2012, paper JT2A.47 DOI:10.1364/HILAS.2012.JT2A.47

[5] B. Marchetti *et al.*, "Conceptual and Technical Design Aspects of Accelerators for External Injection in LWFA", *Appl. Sci.*, vol. 8, p. 757, May 2018. DOI:10.3390/app8050757

[6] M. Felber, M. Hoffmann, U. Mavric, H. Schlarb, S. Schulz, and W. Jalmuzna, "Laser Synchronization at REGAE using Phase Detection at an Intermediate Frequency", in *Proc. 3rd Int. Particle Accelerator Conf. (IPAC'12)*, New Orleans, LA, USA, May 2012, paper WEPPD048, pp. 2624–2626.

[7] F. B. Kiewiet *et al.*, "Femtosecond synchronization of a 3GHz RF oscillator to a mode-locked Ti:sapphire laser", *Nucl. Instr. Meth.*, vol. 484, pp. 619–624, 2002, DOI:10.1016/S0168-9002(01)01994-5.

[8] M. Titberidze *et al.*, "Present and Future Optical-to-Microwave Synchronization Systems at REGAE Facility for Electron Diffraction and Plasma Acceleration Experiments", in *Proc. 6th Int. Particle Accelerator Conf. (IPAC'15)*, Richmond, VA, USA, May 2015, pp. 833–836. DOI:10.18429/JACoW-IPAC2015-MOPHA026

[9] M. Titberidze, M. Felber, T. Lamb, H. Schlarb, C. Sydlo, and R. A. Loch, "Fs Level Laser-to-RF Synchronization at REGAE", in *Proc. 8th Int. Particle Accelerator Conf. (IPAC'17)*, Copenhagen, Denmark, May 2017, pp. 3972–3975. DOI:10.18429/JACoW-IPAC2017-THPAB109

[10] L. R. Doolittle, M. S. Champion, and H. Ma, "Digital Low-Level RF Control Using Non-IQ Sampling", in *Proc. 23rd Linear Accelerator Conf. (LINAC'06)*, Knoxville, TN, USA, Aug. 2006, paper THP004, pp. 568–570.

[11] M. Felber *et al.*, "Compact MTCA.4 Based Laser Synchronization", in *Proc. 5th Int. Particle Accelerator Conf. (IPAC'14)*, Dresden, Germany, Jun. 2014, pp. 1823–1825. DOI:10.18429/JACoW-IPAC2014-TUPRI107

[12] E. Ivanov, S. Diddams and L. Hollberg, "Study of the Excess Noise Associated with Demodulation of Ultra-Short Infrared Pulses", *IEEE Transactions on Ultrasonics, Ferroelectrics,and Frequency Control*, vol. 52, pp. 1068–1074, 2005, DOI:10.1109/TUFFC.2005.1503992.

[13] W. Zhang, *et al.*, "Amplitude to phase conversion of InGaAs PIN photodiodes for femtosecond lasers microwave signal generation", *Appl. Phys. B. Laser and Optics,*, vol. 106, no. 2, pp. 301–308, 2012, DOI:10.1007/s00340-011-4710-1.

[14] A. Gliserin, M. Walbran, and P. Baum "Passive optical enhancement of laser-microwave synchronization" *Appl. Phys. Lett.*, vol. 103, p. 031113, 2013. DOI:10.1063/1.4815929

[15] M. Titberidze, "Pilot Study of Synchronization on a Femtosecond Scale between the Electron Gun REGAE and a Laser-Plasma Accelerator", Ph.D. thesis, Phys. Dept., University of Hamburg, Hamburg, Germany, 2017. DOI:10.3204/PUBDB-2017-11374

[16] M. Felber *et al.*, "Implementation of MTCA.4-based Controls for the Pulsed Optical Synchronization Systems at DESY", in *Proc. 37th Int. Free Electron Laser Conf. (FEL'15)*, Daejeon, Korea, Aug. 2015, paper MOP040, pp. 115–117, DOI:10.18429/JACoW-FEL2015-MOP040.